



## UvA-DARE (Digital Academic Repository)

### **MOLAB, a mobile facility suitable for non-invasive in-situ investigations of early and contemporary paintings: case study – Victory Boogie Woogie (1942–1944) by Piet Mondrian**

Miliani, Costanza; Sgamellotti, Antonio; Kahrim, K.; Brunetti, Brunetto ; Aldovandri, A.; van Bommel, M.R.; van den Berg, K.J.; Janssen, H.

**Publication date**

2008

**Document Version**

Final published version

**Published in**

ICOM-CC triennial meeting

[Link to publication](#)

**Citation for published version (APA):**

Miliani, C., Sgamellotti, A., Kahrim, K., Brunetti, B., Aldovandri, A., van Bommel, M. R., van den Berg, K. J., & Janssen, H. (2008). MOLAB, a mobile facility suitable for non-invasive in-situ investigations of early and contemporary paintings: case study – Victory Boogie Woogie (1942–1944) by Piet Mondrian. In *ICOM-CC triennial meeting* (pp. 244-251). ICOM-CC.

**General rights**

It is not permitted to download or to forward/distribute the text or part of it without the consent of the author(s) and/or copyright holder(s), other than for strictly personal, individual use, unless the work is under an open content license (like Creative Commons).

**Disclaimer/Complaints regulations**

If you believe that digital publication of certain material infringes any of your rights or (privacy) interests, please let the Library know, stating your reasons. In case of a legitimate complaint, the Library will make the material inaccessible and/or remove it from the website. Please Ask the Library: <https://uba.uva.nl/en/contact>, or a letter to: Library of the University of Amsterdam, Secretariat, Singel 425, 1012 WP Amsterdam, The Netherlands. You will be contacted as soon as possible.

UvA-DARE is a service provided by the Library of the University of Amsterdam (<https://dare.uva.nl>)

*Abstract*

This paper intends to demonstrate MOLAB's multi-technique *in-situ* non-invasive approach as applied to the study of the materials found in Mondrian's painting, *Victory Boogie Woogie*, conserved at the Gemeentemuseum, The Hague. The study was carried out using five portable spectroscopic techniques; x-ray fluorescence, mid-infrared reflectance spectroscopy, near infrared reflectance spectroscopy, UV-vis spectroscopy in absorption and emission modes and fluorescence imaging, allowing for the identification of the pigments employed by Mondrian in his last unfinished masterpiece. Signature key elements belonging to each of the colours employed by Mondrian along with the clean lines and restricted palette of the artist allowed for a greater elaboration of the build-up of the work.

*Résumé*

L'article a pour objectif d'expliquer l'approche multi-technique *in situ* non invasive de MOLAB telle qu'elle a été utilisée pour l'examen des matériaux trouvés dans le tableau de Mondrian *victory boogie woogie*, qui est conservé au Gemeente museum de La Haye. Cet étude a été menée avec l'utilisation de cinq techniques de spectroscopie portable; fluorescence de rayons X, spectroscopie de réflexion dans l'infrarouge moyen, spectroscopie de réflexion proche infrarouge, spectroscopie UV-VIS dans les modes d'absorption et d'émission, et imagerie de fluorescence, permettant d'identifier les pigments employés par Mondrian dans son dernier chef-d'œuvre inachevé. Les éléments clés des signatures appartenant à chacune des couleurs utilisées par Mondrian outre ses lignes propres et sa palette confidentielle ont permis une meilleure mise au point du rassemblement de son œuvre.

*Synopsis*

Este documento pretende mostrar el método no invasivo multitécnico MOLAB *in situ* tal y como se aplicó en el estudio de los materiales encontrados en el cuadro de Mondrian, *Victory Boogie Woogie*, conservado en el museo Gemeentemuseum, La Haya. El estudio se llevó a cabo empleando cinco técnicas espectroscópicas portátiles: fluorescencia de rayos-X, espectroscopia reflectante infrarroja media,

MOLAB, a mobile facility suitable for non-invasive *in-situ* investigations of early and contemporary paintings: case study – *Victory Boogie Woogie* (1942–1944) by Piet Mondrian

C Miliani\* and A Sgamellotti  
Centre SMAArt and CNR-ISTM  
Universita' di Perugia  
Perugia, Italy  
Tel.: +390755855639  
Fax: +390755855606  
E-mail: miliani@thch.unipg.it

K Kahrin and B G Brunetti  
Centre SMAArt and Dipartimento di Chimica  
Universita' di Perugia  
Perugia, Italy

A Aldrovandi  
Opificio delle Pietre Dure  
Firenze, Italy

M R van Bommel and K J van den Berg  
ICN, Amsterdam  
The Netherland

H Janssen  
Gemeentemuseum  
Den Haag, The Netherland

\*Author for correspondence

*Keywords*

modern paintings, non-invasive, Piet Mondrian, x-ray fluorescence, mid-infrared reflectance spectroscopy, near infrared reflectance spectroscopy, UV-vis fluorescence

**Introduction**

Scientific examination of artwork is generally carried out by micro-samplings that allow scientists to characterise the nature and behavior of inorganic and organic materials using advanced laboratory analytical techniques. Although excellent results may be obtained by this approach, the necessity to maintain an integral painting surface often limits potential micro-sampling to the lateral borders of the artwork or, as in the case of small and well conserved works, may be totally prohibited.

In recent years, multi-technique non-invasive *in-situ* investigations have been carried out on several mural, panel and canvas paintings but, thus far, have not been applied to the study of modern or contemporary works with the exception of few investigations involving the limited application of a single technique (Zieske 1995, Bacci et al. 2003).

Indeed, modern and contemporary works present conditions, such as a seemingly good state of conservation and visible integrity that favour the non-invasive approach. But difficulty in employing these techniques is encountered due to the complexity, in both number and nature, of the synthetic and natural materials employed from the 20th century onwards.

This paper reports an exemplary non-invasive, multi-technique study of *Victory Boogie Woogie* (1942–1944) by Piet Mondrian carried out by MOLAB. The facility consists of portable instrumentation available for non-invasive

espectroscopia reflectante infrarroja cercana, espectroscopia UV-vis en modos de absorción y emisión y representación óptica por fluorescencia, permitiendo la identificación de los pigmentos empleados por Mondrian en su última obra maestra inacabada. Los elementos clave de signatura pertenecientes a cada uno de los colores empleados por Mondrian junto con los limpios trazados y la reducida escala de colores del artista permitió una mejor elaboración de la restauración del trabajo.

measurements on site where the artwork is located or exhibited. This eliminates risks and costs associated with the transportation to and from a laboratory. The service is offered to European scientists and conservator/restorers through Eu-ARTECH, an I3 initiative of the 6th Framework Program of the EU (<http://www.eu-artech.org>).

*Victory Boogie Woogie* is Piet Mondrian's last work and recognised as one of the most important emblems of abstract or non-figurative art in the 20th century. Mondrian was still executing this painting upon his death in New York, 1944. The unfinished work was sold to an American collector by his descendants. In 1988, the work was purchased by the Dutch state and may now be seen on permanent display in the Gemeentemuseum, The Hague. The unfinished character of the work presents a rare insight into Mondrian's late painting techniques. To capitalise on this unique opportunity a wide number of investigations have been planned as part of an exemplary synergistic project uniting curators, conservators and scientists.

## Experimental

The analysis of Mondrian's painting took place in the exhibition room of the Gemeentemuseum, which allowed both visitors and press a rare opportunity to follow the experiments. To facilitate analysis, the canvas had been positioned vertically on an easel directly behind a bench top supporting the instrumentation. The painting has a distinctive lozenge shape ( $127 \times 127$  cm<sup>2</sup>, vertical axis 179 cm) and is composed of more than 500 rectangles of different colours and composition. These were all numbered to help in identifying analysed areas. During the five days of access, about 220 areas were investigated, each time avoiding contact with the painting's surface.

*Reflectance mid-infrared (mid-FTIR)* – Spectra were acquired using a portable JASCO VIR 9500 spectrophotometer equipped with a Remspec mid-infrared fibre optic sampling probe. The probe is made of chalcogenide glass that allows the collection of spectra in the range  $4000\text{--}900$  cm<sup>-1</sup> at a resolution of 4 cm<sup>-1</sup>. The width of the investigated area, determined by the probe diameter, is circa 4 mm.

*Reflectance near-infrared (near-FTIR)* – Near infrared spectra were recorded with a portable JASCO VIR 9600 spectrophotometer. The spectral range is  $12500$  cm<sup>-1</sup> –  $4000$  cm<sup>-1</sup> with a resolution of 4 cm<sup>-1</sup>. The spectrophotometer is equipped with a silica glass fibre optic Y sampling probe that has a spatial resolution of about 10 mm<sup>2</sup>.

*Reflectance fluorimetry (RF)* – UV-vis emission spectra were collected by a portable fluorimeter prototype. The spectral resolution is about 20 nm using a 600 μm fibre optic diameter. The fibre allows for analysis of a surface area of 2 mm<sup>2</sup>.

*X-ray fluorescence (XRF)* – XRF instrumentation consists of a miniaturised x-ray generator, EIS P/N 9910, equipped with a tungsten anode and a silicon drift detector (SDD). The resolution is about 150 eV at 5.9 keV. It allows the detection of elements with  $Z > 14$ . The sample-detector distance was fixed at 2 cm resulting in a beam diameter of 4 mm. A procedure fitting has been employed for calculating the counts per seconds (cps) for each element.

*Fluorescence imaging* – Fluorescence was excited by two Lubino lamps with a maximum emission at 365 nm equipped with additional filters (Schott Dug11) to eliminate the visible component of light. To evaluate the quality of the image and to correct for spurious light, a reflectance reference (Spectralon 99%) was used. Images were recorded with a digital Nikon camera.

## Results and discussion

Mondrian was key to artistic tendencies of the 20th century in his evolution from figurative to ever more abstract art. In *Victory Boogie Woogie* blue, yellow,

red and white are interwoven over the entire surface, fragmented into larger and smaller planes and small blocks of colour. The lozenge-shaped painting was covered with loosely attached bits of colored paper and plastic, which Mondrian used to experiment with changes in his composition. It is generally believed, though still under some debate, that these tapes were meant to be ultimately replaced by a painted version of the fragmented lines. Despite the simplicity in the artist's choice of colours, the palette composition was complex due to mixtures and heterogeneities not always discernable by eye.

*White* – The fluorescence image of the surface revealed that, contrary to their appearance, the white rectangles were not homogeneous in composition. As an example, the fluorescence image of rectangles 289 reveals yellow and grey spots on a bluish background (Figure 1 inserts a and b). UV-vis fluorescence spectral analysis of the white paint reveals the presence of two different emission spectra. In the majority of cases this was characterised by a maximum at 430 nm. A strong and sharp band at 380 nm was observed only in correspondence with yellow fluorescing areas (Figure 1). This near-band-edge emission is a peculiar property of ZnO due to an excitation transition and hence largely unaffected by impurities or defects of its structure (Reynold et al. 2000).

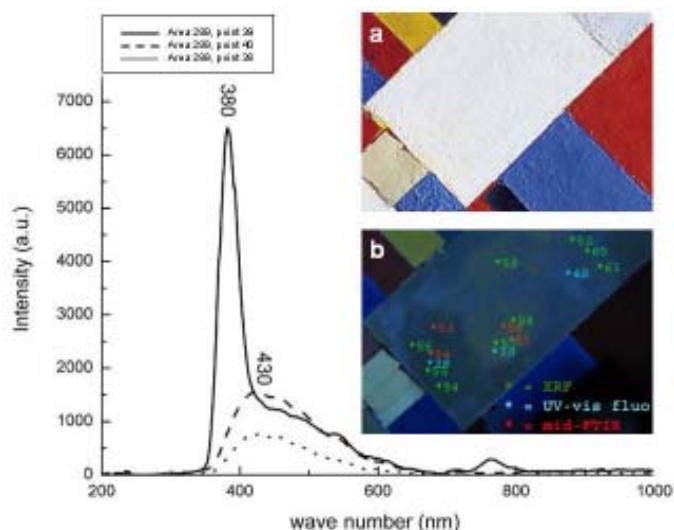


Figure 1. UV-vis fluorescence emission spectra of a white rectangle (289). Inserts show: a) visible light image b) UV-fluorescence image of rectangle 289

The XRF peak fitting procedure adopted for white paint spectra revealed the presence of three elements possibly related to white pigments; Zn, Ba and Ti. At 4.5 and 4.9 keV, the barium L electron transitions overlap those due to the titanium K electron transitions. In order to resolve the two contributions, the mean ratio of Ba  $L_{\alpha}/L_{\beta}$  and Ti  $K_{\alpha}/K_{\beta}$  peak intensities were measured for a number of standard spectra of pure barium sulphate and titanium dioxide using identical experimental parameters. Results of the fitting procedure are reported in Table 1.

Titanium and barium can be related to the use of titanium dioxide and barium sulphate, the later also identified by its mid-FTIR spectroscopy characteristic absorption bands at 1075, 1120 and 1185  $\text{cm}^{-1}$ . The discrimination between zinc oxide and zinc sulphide is far more complicated as their distinctive absorption bands fall between 500 and 400  $\text{cm}^{-1}$ , a spectral region where the chalcogenide glass fibre is not transparent. Nevertheless UV-vis fluorescence data proved that ZnO is restricted to select areas, mainly on the external triangles and on triangle 2 near the top of the lozenge. The emission at 430 nm, typical of all other white areas, is in accordance with the reported luminescence property of zinc sulphide caused by the recombination of electron with trapped hole at  $VZn'$  and  $VZn''$  (Yoon et al. 2001).

Table 1. Results of fitting of XRF spectra on white areas, expressed as counts per second

|            | Area | S(K $\alpha$ ) | Ca(K $\alpha$ ) | Ti(K $\alpha$ ) | Ba(L $\alpha$ ) | Co(K $\alpha$ ) | Zn(K $\alpha$ ) | Pb(L $\alpha$ ) | Se(K $\alpha$ ) | Sr(K $\alpha$ ) | Cd(K $\alpha$ ) |
|------------|------|----------------|-----------------|-----------------|-----------------|-----------------|-----------------|-----------------|-----------------|-----------------|-----------------|
| VBW_X_22_w | 2    | 4              |                 | 290             | 234             | 2               | 565             |                 |                 | 16              |                 |
| VBW_X_23_w | 10   | 3              |                 | 276             | 226             | 1               | 551             |                 |                 | 26              |                 |
| VBW_X_25_w | 2    | 3              | tr              | 306             | 254             | 3               | 609             |                 |                 | 22              |                 |
| VBW_X_32_w | 31   | 4              | tr              | 272             | 248             |                 | 613             |                 | tr              | 24              | 19              |
| VBW_X_33_w | 31   | 5              | tr              | 286             | 264             |                 | 657             |                 |                 | 25              | tr              |
| VBW_X_44_w | 31   | 9              |                 | 539             | 491             |                 | 1220            | tr              |                 | 48              | tr              |
| VBW_X_45_w | 31   | 6              |                 | 486             | 464             |                 | 1168            |                 |                 | 47              |                 |
| VBW_X_46_w | 31   | 6              | tr              | 483             | 453             |                 | 1129            |                 |                 | 44              |                 |
| VBW_X_47_w | 31   | 7              |                 | 508             | 467             |                 | 1163            |                 | 11              | 46              | 149             |
| VBW_X_48_w | 31   | 8              | tr              | 458             | 445             |                 | 1102            |                 |                 | 42              |                 |
| VBW_X_49_w | 114  | 5              |                 | 570             | 442             |                 | 1125            |                 |                 | 56              |                 |
| VBW_X_50_w | 31   | 7              | tr              | 480             | 442             |                 | 1123            |                 |                 | 46              | tr              |
| VBW_X_51_w | 31   | 7              | tr              | 443             | 419             |                 | 1028            | tr              |                 | 39              |                 |
| VBW_X_54_w | 289  | 6              | tr              | 419             | 327             |                 | 810             |                 |                 | 39              |                 |
| VBW_X_55_w | 289  | 6              |                 | 413             | 332             |                 | 807             |                 |                 | 39              | tr              |
| VBW_X_56_w | 289  | 5              |                 | 408             | 321             |                 | 793             |                 |                 | 38              |                 |
| VBW_X_57_w | 289  | 7              | tr              | 459             | 353             |                 | 892             |                 |                 | 45              |                 |
| VBW_X_58_w | 289  | 6              | tr              | 453             | 350             |                 | 883             |                 |                 | 46              |                 |
| VBW_X_59_w | 289  | 7              | tr              | 495             | 379             |                 | 943             |                 |                 | 47              |                 |
| VBW_X_60_w | 289  | 6              |                 | 418             | 391             |                 | 972             |                 |                 | 49              |                 |
| VBW_X_61_w | 289  | 8              | tr              | 404             | 399             |                 | 985             |                 |                 | 44              |                 |
| VBW_X_62_w | 289  | 8              |                 | 445             | 428             |                 | 1089            |                 |                 | 48              |                 |
| VBW_X_63_w | 491  | 8              |                 | 500             | 416             |                 | 1001            |                 |                 | 44              |                 |
| VBW_X_64_w | 491  | 7              | 354             | 543             | 429             |                 | 1053            |                 |                 | 45              |                 |
| VBW_X_65_w | 491  | 6              |                 | 455             | 349             |                 | 876             | tr              |                 | 42              | 191             |
| VBW_X_78_w | 222  | 7              |                 | 466             | 454             |                 | 1159            |                 |                 | 48              | 1256            |
| VBW_X_82_w | 493  | 4              | tr              | 290             | 234             |                 | 565             |                 |                 | 16              | 0               |

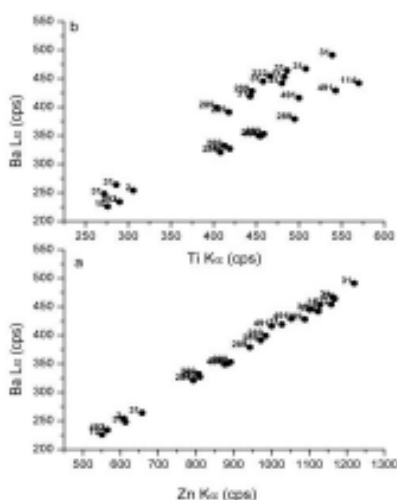


Figure 2. Correlation plots of XRF data for white: a) Ba L $\alpha$  (cps) versus Zn K $\alpha$  (cps), b) Ba L $\alpha$  (cps) versus Ti K $\alpha$  (cps)

Correlation plots for Ti, Ba and Zn counts are shown in Figure 2a. Plotting the Ba L $\alpha$  counts versus the Zn K $\alpha$  counts for all white rectangles results in a very good correlation with R equal to 0.99. Conversely, plotting Ti K $\alpha$  versus Ba L $\alpha$  or Zn K $\alpha$  results in two satisfactory and distinct correlations (Figure 2b). The measured points resulting in a higher content of titanium with respect to the average value are those appearing grey on the fluorescence image, such as X\_61, 62, 63 in Figure 1b.

Merging information obtained from XRF, mid-FTIR and UV-vis fluorescence, it is possible to conclude that there are three different types of white pigment: a mixture of a Zn-compound (probably ZnS) and barium sulphate, titanium white used in two different concentrations with respect to barium sulphate and zinc white that is restricted to localised spots. It is of interest to report that, exclusively on spots showing the ZnO emission at 380 nm, mid-FTIR spectra revealed two sharp signals at 1540 cm $^{-1}$  ( $\nu_{as}(\text{COO}^-)$ ) and 1400 cm $^{-1}$  ( $\nu_s(\text{COO}^-)$ ) indicative of a probable formation of metal carboxylates (Figure 3a) (Zelenak et al. 2007).

It must be reported that neither lithopone nor zinc sulphide have been identified on Mondrian's so-called Trans-Atlantic paintings, whereas titanium dioxide, barium sulphate, lead white and zinc oxide are usually detected. This emphasises a need to confirm the non-invasive data by means of micro-destructive XRD or Raman.

*Grey* – The elemental composition of grey areas was quite similar to that of white, with the presence of Ti, Ba and Zn. The correlation of Ba versus Zn is the same as that found for white areas, whereas the ratio Ti/Ba is as for

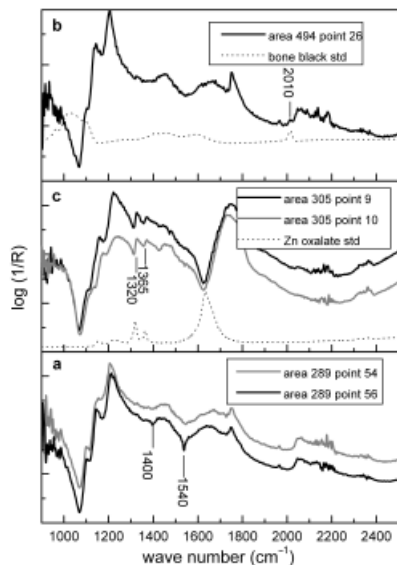


Figure 3. Mid-FTIR spectra of a) two white areas of rectangle 289 (see Figure 1), b) a grey rectangle, c) two areas of a yellow rectangles (see Figure 4). Bone black and zinc oxalate standard spectra recorded in transmission mode are reported as dotted lines

white areas richest in titanium. Mid-FTIR spectroscopy allowed for the identification of bone black by its characteristic small sharp signal at  $2010\text{ cm}^{-1}$  (Miliani et al. 2007) visible in Figure 3b.

**Blue** – Blue areas were generally characterised by the absence of heavy elements related to most blue pigments and by the presence of kaolinite,  $\text{Al}_4[\text{Si}_4\text{O}_{10}](\text{OH})_8$ . This is identified by a characteristic sharp band near  $4525\text{ cm}^{-1}$  and  $7070\text{ cm}^{-1}$  (near-FTIR spectra) assigned to the combination mode of internal surface OH groups. These findings suggest the use of synthetic ultramarine, a pigment usually containing residual kaolinite from its synthesis (Landman and de Waal 2004). XRF measurements indicate the additional presence of cobalt on three of the seven analyzed blue squares. This was assigned to cobalt blue ( $\text{CoAl}_2\text{O}_4$ ) by near-FTIR spectra showing a well-structured electronic absorption in the  $6500\text{--}8500\text{ cm}^{-1}$  range (Bacci and Picollo 1996, Miliani et al. 2007). Technical studies of other so-called Trans-Atlantic paintings by Mondrian conducted by micro-destructive analysis report the identification of both artificial ultramarine and cobalt blue (Cooper and Spronk 2001).

**Red** – Red squares were rich in cadmium, selenium and sulphur, suggesting the use of sulfoselenide cadmium red. UV-vis fluorescence spectra showed a broad emission centred at about  $810\text{ nm}$ . Being far from the band edge this value can be assigned to a deep-trap emission resulting from structural defects or impurities. The amount of Ti, Ba and Zn is generally very low on red areas suggesting that the sulfoselenide cadmium red has not been mixed in with white pigments.

A red organic pigment with a strong emission at  $620\text{ nm}$  was detected on several transparent cellophane tapes that were probably painted on the reverse side and glued by Mondrian himself. High Performance Liquid Chromatograph-Mass Spectrometry (HPLC-MS) analysis is planned for the identification of the molecular structure of this synthetic dye.

**Yellow** – Yellow squares were generally characterised by cadmium and sulphur related to the use of a cadmium sulphide pigment ( $\text{CdS}$ ,  $\text{Cd}_x\text{Zn}_{1-x}\text{S}$ ). Interestingly, fluorescence imaging of yellow rectangles showed areas of irregular red fluorescence. To illustrate this, visible illumination and UV fluorescence images are compared in Figures 4a and 4b. Spectral measurements of the fluorescing areas showed an intense emission at about  $700\text{ nm}$ , again related to a deep-trap emission resulting from structural defects or impurities (Figure 4). In the case of  $\text{CdS}$  the luminescence bands located in the  $1.70\text{--}1.86\text{ eV}$

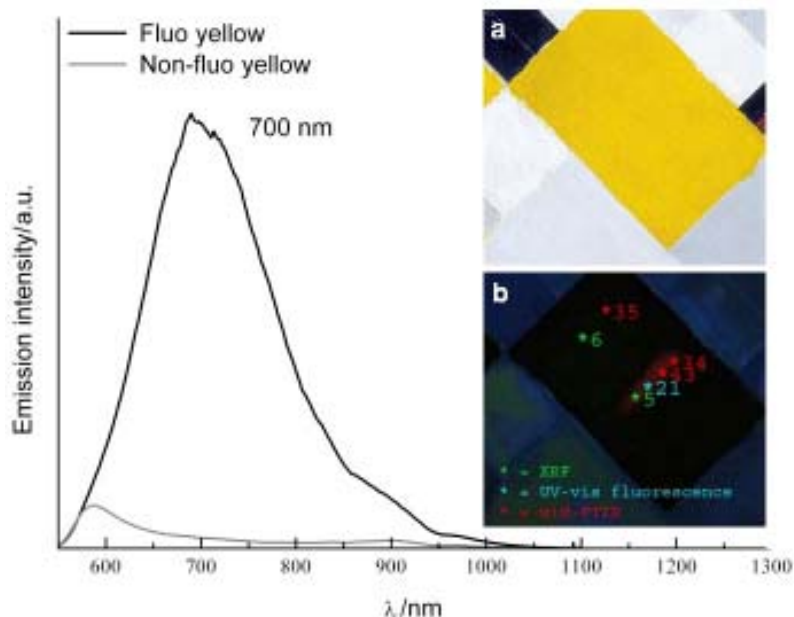


Figure 4. UV-vis fluorescence emission spectra of yellow area. Inserts show detail of a yellow rectangle (564): a) visible light image, b) UV-fluorescence image

range are known as the ‘red’ emission bands, and they have often been attributed to sulphur vacancies (Palafox et al. 1998). Both fluorescing and non-fluorescing yellow areas showed a relevant content of zinc oxalate as revealed by mid-FTIR spectroscopy and demonstrated in Figure 3c. It is not clear if zinc oxalate is an oxidation product or a precursor for the pigment synthesis.

The correlation plot of Cd  $K_{\alpha}$  versus Ba  $L_{\alpha}$  shows that the fluorescent yellow areas present a greater amount of Ba. No other differences between fluorescing and non-fluorescing areas are detectable by elemental analysis (Table 2). This supports Mondrian’s use of two yellow pigments of identical colour but of slightly different composition. The strong UV-vis fluorescence could result from defects undetectable by XRF, while barium could be related to a cadmium yellow lithopone or simply to an addition of barium sulphate to the tube formulation. Since no colour differences were observed and the fluorescing yellow seems to be in the same brush stroke as the non-fluorescing one, it is tempting to think that the two different paints were mixed together on the palette before application. Interestingly, this fluorescing cadmium yellow was found on European paintings by Mondrian and the non-fluorescing cadmium yellow on the Trans-Atlantic paintings (Spronk 2007).

Signature key elements belonging to each of the colours employed by Mondrian along with the clean lines and restricted palette of the artist allowed for some elaboration of the build-up of the work. In certain white areas it was possible to detect the presence of underlying yellow or red not visible, based on small characteristic signals of cadmium or cadmium plus selenium, respectively, in the acquired XRF spectra (Figure 5). In the case of detected cadmium and selenium in a ratio approximating that found in the red areas of the painting, it was concluded that red paint lay beneath the final layer. In the case of detected cadmium but not selenium, both possibilities of underlying red or yellow paint must be taken into consideration as it is possible that selenium may be present in a concentration below the detection limit of the detector. A relevant concentration of Pb was detected in select points analyzed by XRF. These points are not spatially grouped together and fall within areas of different shades and colours. It is believed that these points correspond to

Table 2. Results of fitting of XRF spectra on yellow areas, expressed as counts per second. Letter F indicates points that exhibit fluorescence emission band at 700 nm

|            | Area | S( $K\alpha$ ) | Ti( $K\alpha$ ) | Ba( $L\alpha$ ) | Ni( $K\alpha$ ) | Zn( $K\alpha$ ) | Pb( $L\alpha$ ) | Se( $K\alpha$ ) | Cd( $K\alpha$ ) |
|------------|------|----------------|-----------------|-----------------|-----------------|-----------------|-----------------|-----------------|-----------------|
| VBW_X_02_y | 538  | 34             |                 | 7               | 9               | 1349            |                 | 12              | 4474            |
| VBW_X_03_y | 538  | 33             |                 | 7               | 10              | 1393            |                 | 10              | 5097            |
| VBW_X_04_y | 538  | 31             | 6               | 9               | 5               | 1489            |                 | 7               | 880             |
| VBW_X_05_y | 564F | 28             | 34              | 145             | 11              | 1371            |                 | 9               | 5195            |
| VBW_X_06_y | 564  | 36             | tr              | 5               | 6               | 1526            | 7               | 11              | 5064            |
| VBW_X_19_y | 492  | 11             | tr              | 4               | tr              | 496             |                 | tr              | 1487            |
| VBW_X_20_y | 492  | 10             | tr              | tr              | tr              | 431             |                 | tr              | 1398            |
| VBW_X_26_y | 3    | 10             | 0               | tr              |                 | 411             |                 |                 | 1339            |
| VBW_X_34_y | 115F | 9              | 9               | 37              |                 | 436             |                 |                 | 1538            |
| VBW_X_35_y | 115  | 9              | 0               | tr              |                 | 480             |                 |                 | 1567            |
| VBW_X_40_y | 15F  | 7              | tr              | 16              |                 | 442             |                 | tr              | 1345            |
| VBW_X_41_y | 15   | 9              |                 | tr              |                 | 477             |                 | tr              | 1605            |
| VBW_X_79_y | 305  | 23             |                 | 6               | 7               | 1315            |                 |                 | 4734            |
| VBW_X_80_y | 305  | 39             |                 | 8               | 10              | 1867            |                 |                 | 6801            |
| VBW_X_81_y | 305  | 53             |                 | 11              | 10              | 2554            |                 |                 | 8875            |
| VBW_X_84_y | 375F | 13             | 16              | 50              | tr              | 756             | tr              | 5               | 2795            |
| VBW_X_85_y | 375  | 14             | tr              | tr              | 4               | 774             |                 | tr              | 2770            |
| VBW_X_86_y | 117F | 13             | 10              | 67              | 4               | 643             |                 | 20              | 3152            |
| VBW_X_87_y | 117  | 14             |                 | tr              | 6               | 711             |                 | tr              | 2960            |

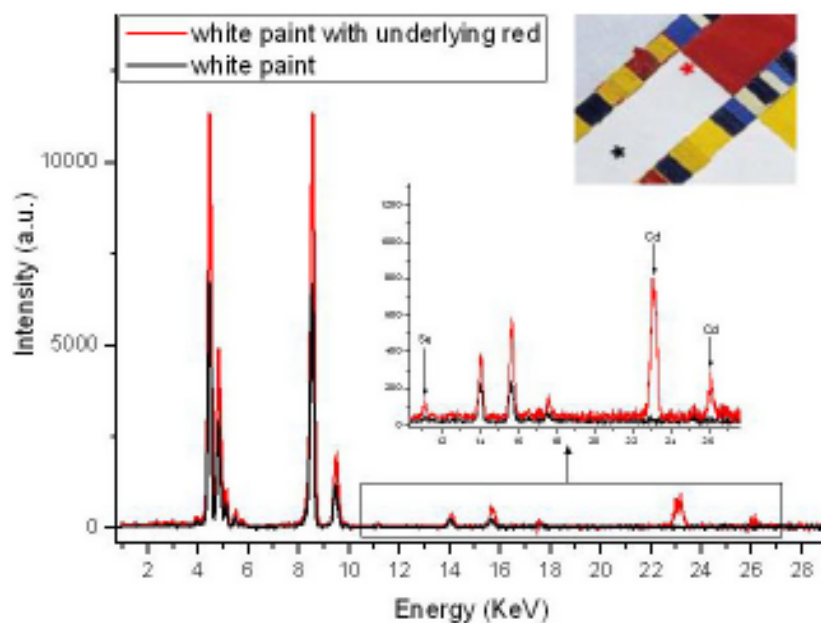


Figure 5. Detail and XRF spectra illustrating the identification of underlying red paint in white rectangle

areas where Mondrian, instead of applying paint layer over paint layer, first scraped away the existing paint before applying the newly desired layer, and in so doing thinned the summed paint stratigraphy to such an extent that x-rays are able to penetrate to the Pb rich canvas priming.

## Conclusion

This study demonstrates that the quantity and the quality of the information that can be obtained using the MOLAB *in-situ* non-invasive multi-technique approach qualifies as an important and valuable method for the technical study of painting materials in contemporary art. It offers the opportunity for extensive analysis of paintings, giving substantial information on material composition and its surface distribution, even in the presence of complex synthetic artists' materials. Moreover, the *in-situ* analysis allows for a synergetic collaboration among scientists, conservators and curators, ever more important when addressing new issues arising from modern and contemporary art.

Different types of white (titanium dioxide, lead white, barium sulphate, zinc oxide and probably zinc sulphide), blue (cobalt blue and synthetic ultramarine), red (sulfoselenide cadmium red and an organic dye) and yellow (fluorescent and non-fluorescent cadmium sulphide) pigments have been identified. The signature key elements belonging to individual colours of Mondrian's palette, in several cases, allowed for the identification of yellow or red strips under white squares by the detection of small characteristic signals of cadmium or cadmium plus selenium, respectively. These observations may prove to be relevant to curators for a better understanding of the painting's construction and in revealing earlier phases of the artist's composition.

In spite of the numerous results obtained through the non-invasive approach, unquestionably, micro-sampling remains essential in examining stratification of materials or to identify certain organic compounds with precision. In the present case study, where sampling is not permitted, we will be taking advantage of some recovered paint fragments, lost from edges, where consolidation was no longer possible. These fragments will be studied by microscopy and SEM-EDS to establish the stratigraphy. XRD or Raman will be employed to confirm the presence of both ZnO and ZnS, whereas HPLC-MS analysis is planned for the identification of the organic red dye emitting at 620 nm.



## Acknowledgements

The work has been carried out through the support of the EU within the 6th Framework Programme (Contract Eu-ARTECH, RIII3-CT-2004-506171). Authors gratefully acknowledge the staff of the MOLAB Transnational Access.

## References

- Bacci, M and Picollo, M. 1996. Non-destructive detection of Co(II) in paintings and glasses. *Studies in Conservation* 41, 136–144.
- Bacci, M, Casini, A, Cucci, C, Picollo, M, Radicati, B and Vervat, M. 2003. Non-invasive spectroscopic measurements on the *Il ritratto della figliastra* by Giovanni Fattori: identification of pigments and colourimetric analysis. *Journal of Cultural Heritage* 4(4), 329–336.
- Cooper, H and Spronk, R. 2001. *Mondrian: The Transatlantic Paintings*. Yale University Press.
- Landman, A A and de Waal, D. 2004. Fly Ash as a Potential Starting Reagent for the Synthesis of Ultramarine Blue. *Materials Research Bulletin* 39(4–5), 655–667.
- Miliani, C, Rosi, F, Burnstock, A, Brunetti, B G and Sgamellotti, A. 2007. Non-invasive in-situ investigations versus micro-sampling: a comparative study on a Renoirs Painting. *Applied Physics A* 89(4), 849–856.
- Palafox, A, Romero Paredes, G, Maldonado, A, Asomoza, R, Acosta, D R and Palacios Gómez, J. 1998. Physical properties of CdS in thin films obtained by chemical spray over different substrates. *Solar Energy Material and Solar Cells* 55, 31.
- Reynold, D C, Look, D C, Jogai, B and Hoelscher, J E. 2000. Time-resolved photoluminescence lifetime measurements of the  $\Gamma_5$  and  $\Gamma_6$  free excitons in ZnO. *Journal Applied Physics* 88(4), 2152–2153.
- Spronk, R. 2007. Personal communication.
- Yoon, K H, Ahn, J K and Cho, J Y. 2001. Optical characteristics of undoped and Mn doped ZnS films. *Journal of Materials Science* 36 (6), 1373–1376.
- Zelenak, V, Vargova, Z and Gyoryova, K. 2007. Correlation of infrared spectra of zinc(II) carboxylates with their structures *Spectrochimica Acta Part A* 66 (2), 262–272.
- Zieske, F. 1995. An investigation of Paul Cézanne's watercolors with emphasis on emerald green. *The Book and Paper Group Annual* 14, 105–115.